Electric Power Systems Research 163 (2018) 348–355

Contents lists available at ScienceDirect

Electric Power Systems Research

journal homepage: www.elsevier.com/locate/epsr

A novel control scheme to reduce the reactive power processed by a Multifunctional Voltage-Quality Regulator

J.C. da Cunha[a], R.T. Hock Jr.[a], S.V. Garcia Oliveira[a], L. Michels[b], M. Mezaroba[a,*]

[a] Santa Catarina State University, Brazil
[b] Federal University of Santa Maria, Brazil

ARTICLE INFO

Keywords:
APF
DSTATCOM
Multifunctional converter
Power quality
Voltage regulation
Reactive power reduction

ABSTRACT

Solving voltage regulation in underrated grid networks can be very time consuming and costly for operators and unpleasant for customer, who constantly experience equipment malfunctions due poor voltage quality. Active solutions such as Multifunctional Voltage-Quality Regulator (MVQR) work well as a quick fix in these cases, bringing voltages to the right levels as soon as installed, feeding active or reactive power into their point of connection. Unfortunately, current solutions can be fastidious, adjusting voltage levels that are already adequate for customer services to a specific fixed setpoint, unnecessarily spending energy, overusing distribution networks, wearing out energy-storage components and eventually not optimizing the equipment's regulation capacity. To address the aforementioned problems, this manuscript proposes a control scheme to reduce the reactive power processed in an existing MVQR. The MVQR was based in a distribution static compensator (DSTATCOM) with active harmonic filtering feature. Where voltage-magnitude regulation is achieved by reactive power injection only, while harmonic mitigation is performed by harmonic injection based on PCC-voltage-detection-method (PCC-VDM). The proposed MVQR control scheme reduces the reactive energy injection when the voltage level at PCC is within limits of relevant standards. The main contribution of this paper is the detailed mathematic analysis of the scheme for reducting the reactive energy injection, which had not been found in literature. This analysis shows how to design this scheme to obtain better regulation, guarantee dynamic decoupling from other control loops, as well as ensure closed-loop system stability. Simulation and experimental results were carried out for validation of the proposed control method. The proposed MVQR had shown itself an efficient and effective addition, reducing significant processed reactive power using wisely resources, likely available in similar MVQR topologies.

1. Introduction

Low voltage distribution networks can struggle to supply an adequate voltage to consumer when the load demands more than the available infrastructure can supply. Voltage can be designated as inadequate mostly due to its high harmonic content and/or improper amplitude. An example of an issue would be an underrated long distribution grid powering a large load distributed across its extension.

Poor voltage regulation affects not only customer who constantly experiences equipment malfunctioning but also utility companies, who must comply with several power quality requirements, such as regulation of voltage's magnitude and harmonic content [1]. When costs associated to having poor voltage quality are high enough, utilities companies might look for quick solutions, that are able to fix voltage quality issues without demanding major analysis of the system, like locating problematic loads or evaluating the current infrastructure. Thus, active solutions may be chosen as they can offer a fast installation followed by an immediate voltage magnitude correction and harmonic distortion reduction, among other features [2–5]. Nevertheless, in this context, the voltage quality issue is not fixed by any active solution due the fact that a fast installation in a distributed power system does not allow a proper inspection of the system to map loads, line impedance, transformer's characteristics, generators, etc. Therefore, active systems solutions must be narrowed to those who do not require specific load or source information to adjust the voltage quality.

Several different active schemes have been developed to solve voltage-quality issues, such as Active Power Filters (APF) with reactive compensation [6–22], Distribution Static Synchronous Compensators (DSTATCOM) [23,24,47–50], and multifunctional converters [2–4,25–33]. Among these solutions, classified as a Multifunctional

* Corresponding author.
E-mail address: marcello.mezaroba@udesc.br (M. Mezaroba).

https://doi.org/10.1016/j.epsr.2018.07.012
Received 23 January 2018; Received in revised form 27 April 2018; Accepted 10 July 2018

Voltage-Quality Regulators (MVQR), DSTATCOMs with voltage harmonic mitigation at the point of common coupling (PCC) have presented themselves as most suitable solutions for the voltage quality issue in the context presented in the paper.

Control scheme of a MVQR DSTATCOM can be based on voltage or current strategies. A voltage-controlled DSTATCOM directly control the PCC voltage, aiming voltage magnitude regulation, phase balancing, and reduction of voltage's Total Harmonic Distortion (THD) [25,28,34,35,44,45]. On the other hand, a current-controlled DSTATCOM directly controls its output current and indirectly controls the PCC voltage. Although slower than voltage controlled strategies, the current controlled DSTATCOMs present natural protection against transients and a more stable operation [27,29,31,33,37]. As part of the selection of the most suitable design strategy for the voltage quality issue a harmonic mitigation strategy must be chosen.

Strategies for harmonic mitigation of PCC voltages in MVQR can be implemented based on current or voltage detection [11]. Current detection schemes require additional current sensors to measure the current from specific loads or from specific points of the distribution system, that increases the cost and the complexity for the equipment installation as well as is required an evaluation of which sources and loads should be measured. Moreover, it is difficult to determine which is the current from the source and from the loads in grids, mainly in systems with distributed generation (DG). Differently, voltage detection schemes are based on PCC voltage measurements. Although more complex, the main advantage of voltage detection approach is that voltage measurements must always be done to provide synchronization, resulting in a solution with no additional sensors [34,44,45].

Several voltage detection schemes have been presented in literature. Methods based on emulation of resistances presented [11,13,26,36] do not eliminate completely the PCC harmonics. In Ref. [14] a method was presented based on emulation of tuned active filters, of which the main drawback is occurrence of potential resonances due to undesigned loads [18]. Adaptive and non-linear techniques have good performance [4,30,31,37,38], but also have chattering problems and a more complex implementation in comparison to linear techniques. Internal-model based controllers based on resonant [6,29,39] or repetitive controllers [10] have good reference tracking and good rejection of periodic disturbances.

Unfortunately, current suitable solutions for the voltage quality issue inserted in the context presented in this paper can be fastidious, adjusting voltage levels that are already adequate for customer services to a specific fixed setpoint, unnecessarily spending energy, overusing distribution networks, wearing out energy-storage components and eventually not optimizing the equipment's regulation capacity. This problem is addressed by this paper, where an addition of a control scheme is proposed to reduce the reactive power processed in an existing MVQR.

Recently a few papers addressed the reduction of unnecessary reactive power processing in low voltage regulators [34,35,37,44,41,46]. Setting a suitable voltage magnitude at the PCC can lead to great reactive power reduction [34], which has been commonly regulated at 1.00 p.u. [42,43]. However, the PCC voltage magnitude must comply with local standards. American standard ANSI C84.1 defines the adequate voltage range from 0.95 p.u. to 1.05 p.u. [40], while European standard EN 50160 sets a 0.90 p.u. to 1.10 p.u. range [41]. The methods for reactive power reduction presented in Refs. [35] and [37] are formulated with the need of extra sensoring of grid or load currents and grid parameters to determine the suitable PCC voltage magnitude. On the other hand, Ref. [34] presented a method using only the output apparent power to track the PCC voltage magnitude in which the processed power is minimal.

This paper proposes a simple and novel control scheme to reduce the reactive power processed by a Multifunctional Voltage-Quality Regulator (MVQR) as an alternative for methods presented in Refs. [34,35,37]. The technique was implemented in an existing MVQR solution based in a distribution static compensator (DSTATCOM) with active harmonic filtering feature presented in Ref. [51]. The voltage-magnitude regulation was achieved by reactive power injection only, while harmonic mitigation was performed by harmonic injection based on PCC-voltage-detection-method (PCC-VDM). The proposed MVQR control scheme addition reduces the reactive energy injection when the voltage level at PCC is within limits of relevant standards. The main contribution of this paper is the detailed mathematic analysis of the scheme for reduction the reactive energy injection, which had not been found in literature. This analysis shows how to design this scheme to obtain better regulation, guarantee dynamic decoupling from other control loops, as well as ensure closed-loop system stability. Simulation and experimental results were carried out for validation of the proposed control method.

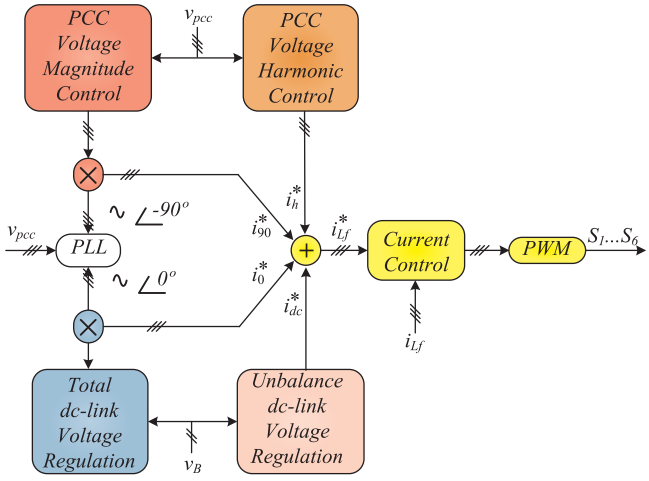

Fig. 1. Block diagram of proposed control for MVQR.

2. Control scheme of proposed MVQR

Proposed PCC voltage regulation scheme is based on a current-controlled DSTATCOM. Fig. 1 presents the basis of proposed scheme, where four outer voltage loops are used for PCC magnitude and harmonics voltage control as well as for dc-link voltage regulation. The combination of the outer voltage loops outputs generate the reference i_{Lf}^* for an inner current control scheme, responsible for the imposition of the injected current on PCC. Fig. 2 presents the proposed three-phase four-wire MVQR control system, where blocks match the colors of Fig. 1 to facilitate the identification of each control loop.

The voltage magnitude and harmonics control at PCC are performed for each phase independently due to three-phase four-wire circuit topology. One can observe that any of the three phases of the inverter can be used for dc-link voltage regulation. However, in order to minimize current unbalance among the phases, the same control action is applied in all the phases to obtain a balanced current of compensation.

PCC voltage magnitude control loop is designed to maintain the magnitude of v_{pcc} within the acceptable limits defined by the grid code. This loop changes the reactive power absorbed or injected in the PCC depending on rms value of v_{pcc}. So the signal i_{90}^* is sinusoidal component in quadrature with v_{pcc}. Additionally, PCC voltage harmonic control loop adds to the current reference signal the content to mitigate the PCC voltage harmonics. The signal i_h^* is generated from a scheme based on the voltage-detection method.

Total dc link voltage control loop is designed for regulation of the sum of voltages across the dc-link capacitors. The dc link voltage regulation is achieved by absorbing or injecting active power from PCC. The magnitude of the sinusoidal v_{pcc} in-phase current reference i_0^* controls the active power exchanged with the PCC. Although not presented in this manuscript, this voltage loop can also be used to control

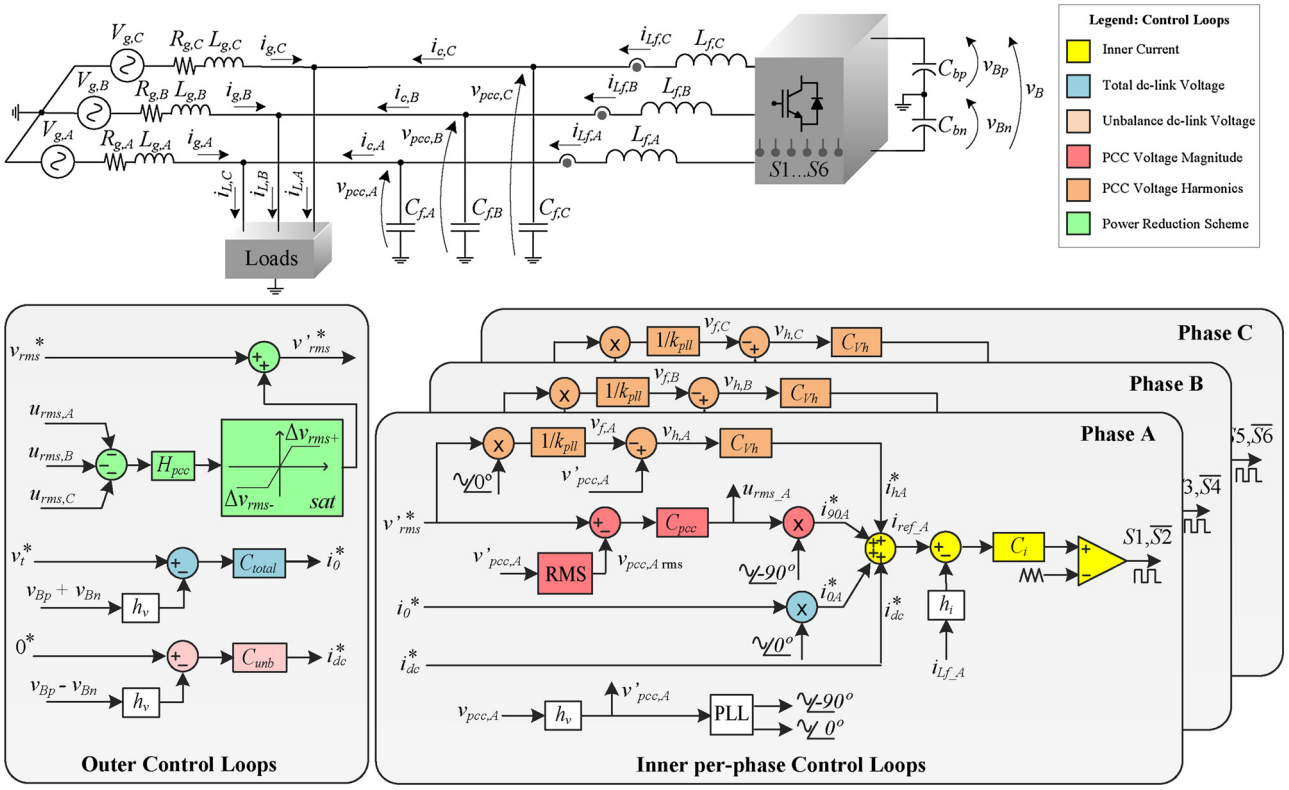

Fig. 2. Block diagram of complete MVQR control system. (For interpretation of the references to color in the text, the reader is referred to the web version of this article.)

active power injected at PCC by a generator or storage systems connected to dc-link.

On the other hand, the unbalance dc link voltage control loop maintains null the difference of voltage between the dc-link capacitors. Voltage balance can be achieved by injecting a small dc current component i_{dc}^{*} to the current reference, where one dc-link capacitor is charged more than the other capacitor.

3. Proposed scheme for reduction of processed reactive power by the MRVQ

PCC voltage magnitude control loop is designed to maintain the magnitude of v_{pcc} within the acceptable limits defined by the grid code from $V_{rms\ \min}$ to $V_{rms\ \max}$. [40,41]. As a result, in most cases it is not necessary that MVQR compensate the voltage magnitude at a constant level, e.g. 1 p.u., because it demands unnecessary extra reactive power compensation. This extra compensation may increase both converter and grid losses.

Fig. 2 presents in green the elements of the proposed scheme for reduction of processed reactive power by the MVRQ. This scheme changes the reference for v_{pcc} reducing or increasing its rms value by Δv_{rms} according to the grid condition but always maintaining v_{pcc} within the acceptable limits. Since control action $u_{\mathrm{rms,A}}$, $u_{\mathrm{rms,B}}$ and $u_{\mathrm{rms,C}}$ are proportional to the magnitude of quadrature component of i_{Lf} injected at PCC, they are directly related to the reactive power processed by MRVQ. Consequently, aiming to reduce the reactive power processed by converter, the control action $u_{\mathrm{rms},T}$ may be lowered as much as possible.

One can observe that positive and negative control action $u_{\mathrm{rms,A}}$, $u_{\mathrm{rms,B}}$ and $u_{\mathrm{rms,C}}$ correspond to capacitive and inductive current compensation at PCC, respectively. Consequently, positive values for $u_{\mathrm{rms},T}$ increases v_{pcc} while negative values decreases v_{pcc}. In order to reduce this control action, a feedback loop is included as highlighted in green in Fig. 2.

The proposed control scheme works as follows. When $u_{\mathrm{rms},ph}$ is positive the control action is generating a capacitive reactive power compensation that increase $v_{pcc,ph}$. As a result, it is possible to reduce the processed reactive power of MVRQ by reducing the reference voltage $v_{rms}'^{*}$. This can be achieved generating Δv_{rms} with negative value by inverting $u_{\mathrm{rms},ph}$ and processing it by the filter H_{pcc}. So, the resulting Δv_{rms} is summed to nominal reference v_{rms}^{*} resulting in a lower new reference $v_{rms}'^{*}$. On the other hand, when $u_{\mathrm{rms},ph}$ is negative the control action is generating a inductive reactive power compensation that decrease $v_{pcc,ph}$. So, the control system works generating a positive Δv_{rms} that is summed to nominal reference v_{rms}^{*} resulting in a higher new reference $v_{rms}'^{*}$.

When this feedback control operates in the linear region, $v_{rms}'^{*}$ can be designed to minimize the reactive power processed by MVQR. On the other hand, the saturation block shown in Fig. 2 forces $v_{rms}'^{*}$ to keep it values within the adequate levels determined by standards. The scheme for reactive power minimization is turned off during saturation, forcing the reference $v_{rms}'^{*}$ be fixed at the lower ($v_{rms} + \Delta v_{rms-}$) or at the higher ($v_{rms} + \Delta v_{rms+}$) acceptable levels.

Fig. 3 presents the equivalent block diagram of proposed scheme assuming that each phase is independent from each other. Fig. 3(a) and (b) shows the equivalent per phase closed-loop systems assuming that the saturation block of Fig. 2 is operating in linear region and under saturation, respectively. The resulting closed-loop transfer function in linear region and under saturation are given by:

$$\frac{V_{pcc,ph}(s)}{V_{rms}^{*}(s)} = \frac{k_{pll}h_i^{-1}C_{pcc}(s)G_{pcc}(s)}{1 + C_{pcc}(s)[h_v k_{pll}h_i^{-1}H_{rms}(s)G_{pcc}(s) + H_{pcc}(s)]} \quad (1)$$

$$\frac{V_{pcc,ph}(s)}{V_{pcc}^{*}(s)} = \frac{k_{pll}h_i^{-1}C_{pcc}(s)G_{pcc}(s)}{1 + h_v k_{pll}h_i^{-1}H_{rms}(s)C_{pcc}(s)G_{pcc}(s)} \quad (2)$$

Fig. 4 presents the frequency response of closed-loop systems given in Eqs. (1) and (2) for system given in Tables 1 and 2.

The low-pass filter $H_{pcc}\ (s) = 1/(2\pi\ 0.05\ \mathrm{s} + 1)$ is employed to

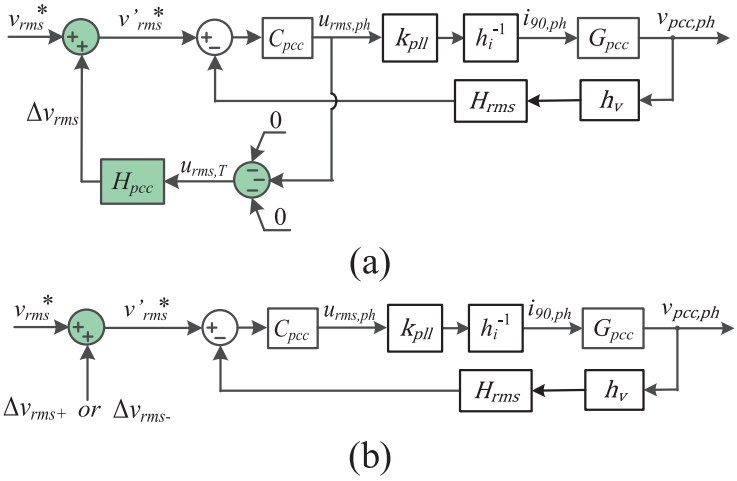

Fig. 3. Proposed scheme for reduction of processed reactive power operating in different conditions. (a) Normal operation. (b) Under saturation.

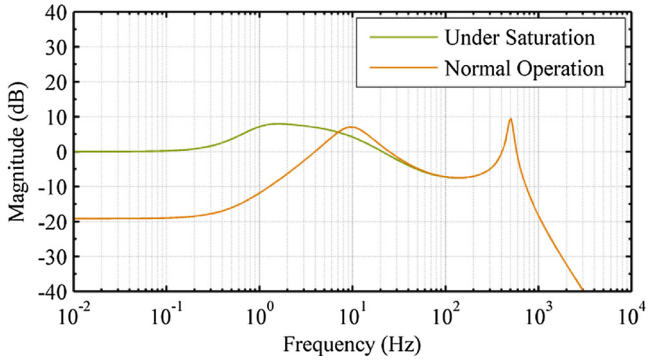

Fig. 4. Frequency response of proposed scheme for reduction of processed reactive under different conditions.

Table 1
MVQR parameters.

Paramerter	Variable	Value
Nominal power	S_o	30 kVA
Nominal dc bus voltage	V_{total}	800 V
Dc bus capacitors	C_{b1} C_{b2}	14,100 μF
Nominal per phase rms voltage	V_{rms}	220 V
Upper limit for rms voltage	$V_{rms\ max}$	231 V
Lower limit for rms voltage	$V_{rms\ min}$	209 V
Grid frequency	f_g	60 Hz
Switching frequency	f_{sw}	20 kHz
Sampling frequency	f_s	20 kHz
Output filter inductance	L_f	560 μH
Output filter capacitance	C_f	50 μF
Grid resistance	R_g	0.75 Ω
Grid inductance	L_g	2 mH
Current sensor gain	h_i	0.068
Voltage sensor gain	h_v	1.000
Peak value pll reference	k_{pll}	$1/110\sqrt{2}$

dynamically decouple the proposed scheme from other inner loops and rms block calculation. In this case, one can observe a poor regulation when the proposed scheme operates in linear region since dc gain is lower than −19 dB. This attenuation can be even enhanced by increasing the dc gain of H_{pcc} (s). As a result, the output $v_{pcc,ph}$ does not track the reference v_{rms}^* but a value closer to $v_{rms}'^*$. On the other hand, when there is saturation, the outer voltage can be considered an constant input offset. As a result, the voltage control tracks with zero steady-state error one of the following references: $v_{rms}'^* = v_{rms} + \Delta v_{rms-}$ or $v_{rms}'^* = v_{rms} + \Delta v_{rms+}$.

Table 2
Manipulated and controlled variables of MVQR.

Control loop	Controlled variable		Manipulated component of i_{Lf}	
	Variable	Freq.	Freq.	Phase
Total dc-link voltage	$v_{Bp} + v_{Bn}$	dc	ω_1	0°
Unbalance dc-link voltage	$v_{Bp} - v_{Bn}$	dc	dc	–
PCC voltage magnitude	v_{pcc}	ω_1	ω_1	90°
PCC voltage harmonics	v_{pcch}	$3\omega_1$, $5\omega_1$, …	$3\omega_1$, $5\omega_1$, …	–

Table 3
Parameters of MRVQ compensators.

Control loop	Parameters
Current control	$C_i(s) = 3793 \times \frac{\frac{s}{816\pi}+1}{s\left(\frac{s}{18,182\pi}+1\right)}$
Total dc-link voltage	$C_{total}(s) = -303 \times \frac{\frac{s}{6\pi}+1}{s\left(\frac{s}{62\pi}+1\right)}$
Unbalance dc link voltage	$C_{unb}(s) = 25 \times \frac{\frac{s}{0.2\pi}+1}{s\left(\frac{s}{2\pi}+1\right)}$
PCC voltage magntitude	$C_{pcc}(s) = 108 \times \frac{\frac{s}{2\pi}+1}{s\left(\frac{s}{20\pi}+1\right)}$
PCC voltage harmonics	$Q = 5000$ $k_{r,3} = 0.0130$ $k_{r,5} = 0.0078$ $k_{r,7} = 0.0052$ $k_{r,9} = 0.0020$ $k_{r,11} = 0.00052$

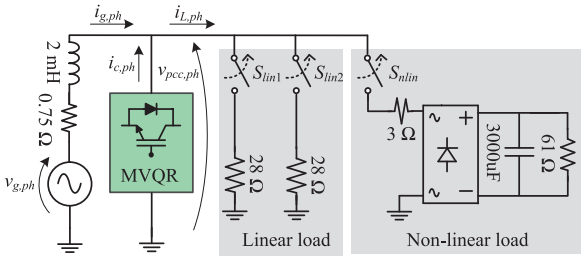

Fig. 5. Single-phase representation of experimental setup.

Table 3 presents the parameters of the compensators used in the MRVQ. In order to simplify the design, the control system was decomposed in independent control loops, where an inner control loop is

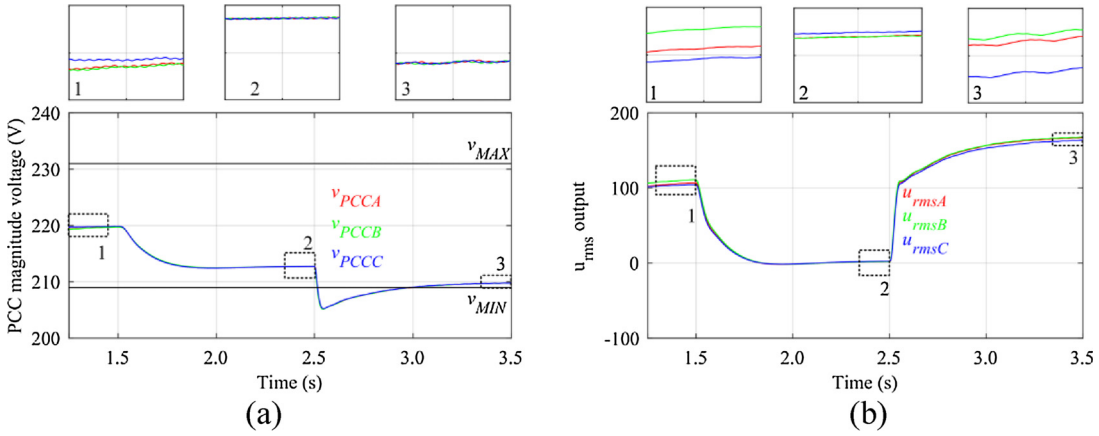

Fig. 6. Simulation results of the reactive power reduction loop response. (a) Magnitude of PCC voltages. (b) Components of reactive power reduction scheme.

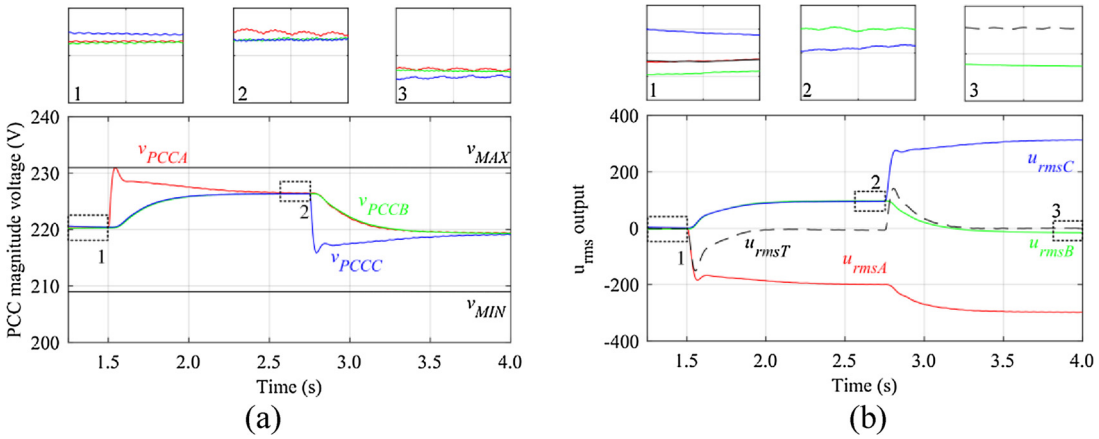

Fig. 7. Reactive power reduction loop response. (a) Magnitude of PCC voltages. (b) Reactive power reduction control actions.

Table 4
Measured values for balanced non-linear loads.

Paramerter	Variable	MVRQ compensator	
		On	Off
PCC voltage — rms	v_{pcc}	212 V	220 V
PCC voltage — THD	$THDv_{pcc}$	6.1%	1.4%
Grid current — rms	i_g	13.1 A	19.7 A
Grid current — THD	$THDi_g$	27.0%	4.5%
Converter current — rms	i_c	0.0 A	12.8 A

dynamically decoupled from outer voltage loops. This assumption is valid assuming that inner control loop has a faster dynamic response in relation to outer ones.

4. Simulations and experimental results

Simulation analysis was used to evaluate the behavior of proposed control scheme for reduction of processed reactive power. Fig. 5 shows the single-phase representation of the test setup, where loads are a combination of linear and nonlinear loads. Three equilibrated resistances comprised linear loads, while three single-phase diode rectifiers with capacitive filter comprised non-linear loads. Balanced loads were used in simulation to match experimental setup. To emulate unbalanced compensation, the voltage source was unbalanced when appropriated, thus having a similar effect of unbalanced loads in the system.

Figs. 6 and 7 show simulation results to demonstrate the performance of proposed scheme for reduction of processed power by MVRQ. The proposed algorithm was designed with $\Delta v_{rms-} = -10$ V and $\Delta v_{rms+} = 10$ V, allowing v_{pcc} voltage deviates from $V_{rms\ \min} + 1$ V to $V_{rms\ \max} - 1$ V (see Table 4). Both simulation results considered balanced non-linear loads only ($S_{lin1} = S_{lin2}$ = off and S_{nlin} = on in Fig. 5).

Simulation shown in Fig. 6 initially considers $v_{g,A} = v_{g,B} = v_{g,C} = 220$ V and proposed scheme for reduction of processed power by MVRQ turned off. Fig. 6(a) shows that the MVRQ initially maintained $v_{pcc} = 220$ V by injecting reactive power, as depicted in Fig. 6(b). At instant $t_1 = 1.5$ s the proposed scheme was turned on, which resulted in a reduction of injected reactive power to almost zero. At instant $t_1 = 2.5$ s a voltage step of -20 V was applied to $v_{g,A}$, $v_{g,B}$, and $v_{g,C}$, when v_{PCC} initially dropped to a value lower than 210 V, this forced the saturation of *sat* block shown in Fig. 2. As a result, the scheme for reduction of processed power by MVRQ became the control structure shown in Fig. 3(b). So MVRQ injected only the necessary reactive power to force v_{pcc} to operate at the lower limit of acceptable voltage range, which is much lower than the power required to force v_{pcc} to operate at a fixed nominal voltage of 220 V.

Simulation shown in Fig. 7 initially considers $v_{g,A} = v_{g,B} = v_{g,C} = 228$ V and the proposed scheme for reduction of processed power by MVRQ turned on. Fig. 7(a) shows that this case resulted in $v_{pcc} \approx 220$ V, without any reactive compensation. At instant $t_1 = 1.5$ s a voltage step of $+20$ V was applied only to $v_{g,A}$. Then the voltage reference for all phases were risen to 226 V in order to maintain a balanced output voltage as well as to minimize the processed reactive power by all three phases. At instant $t_1 = 2.75$ s a voltage step of -20 V is applied in $v_{g,C}$, so the reference dropped to 219.3 V in order to

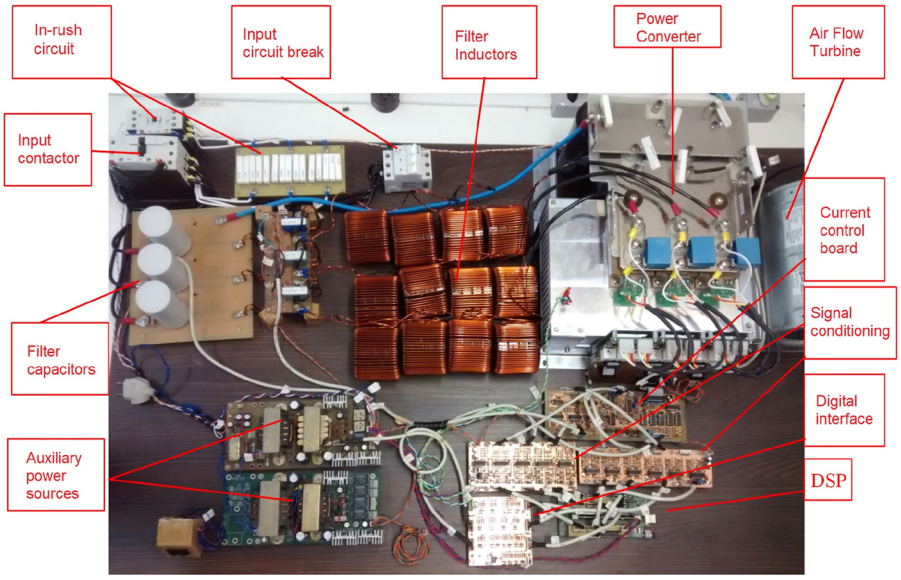

Fig. 8. Picture of built prototype.

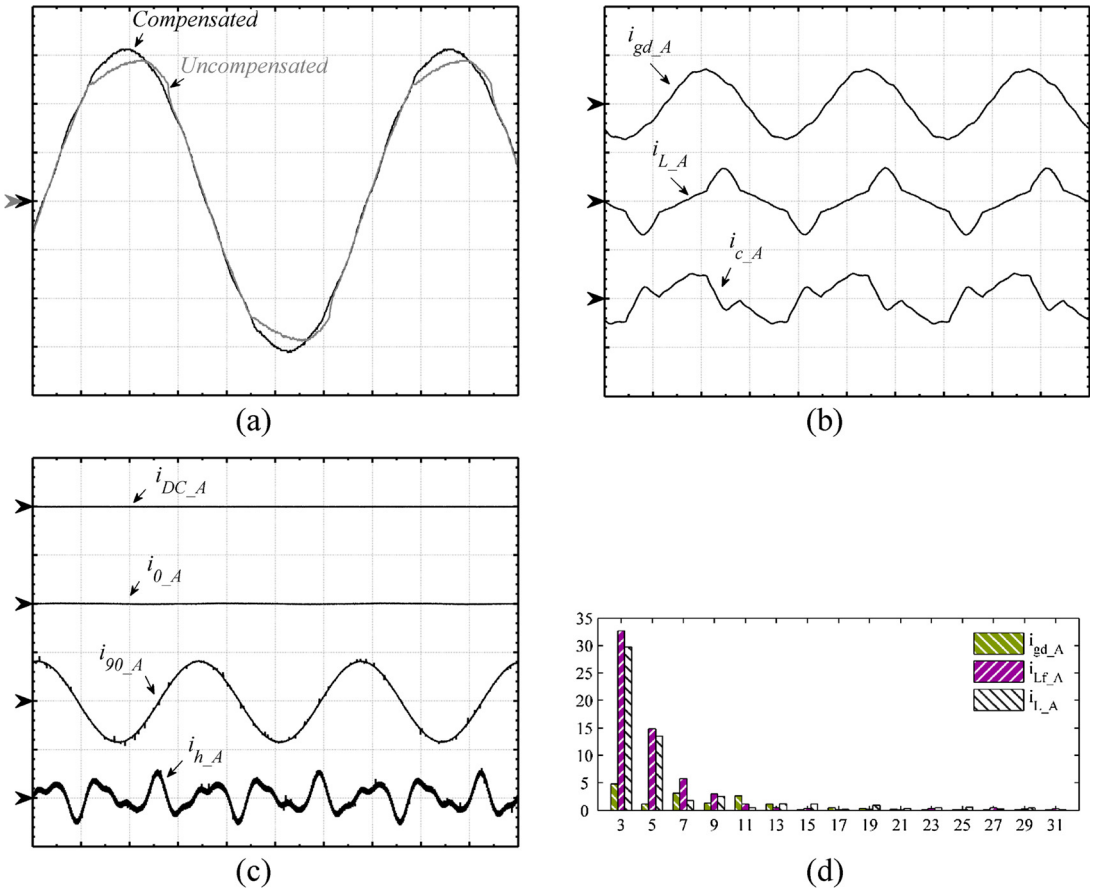

Fig. 9. Experimental results for balanced nonlinear loads at phase A. (a) PCC voltage (100 V/div, 5 ms/div). (b) Grid, load, and converter currents (40 A/div, 5 ms/div). (c) Control components of i_{Lf} (20 A/div, 5 ms/div). (d) Harmonic components of grid, load, and converter currents.

decrease u_{rmsT} up to nearly 0, where $u_{rmsT} = u_{rmsA} + u_{rmsB} + u_{rmsC}$/see Fig. 4.

Aiming to confirm the functionality of the existing MVRQ control scheme and detail the effects of the proposed control addition, a prototype was built based on specifications presented in Table 1. Fig. 8 shows the built prototype.

Fig. 9 presents experimental results for balanced non-linear loads (S_{lin1} = S_{lin2} = off and S_{nlin} = on). Fig. 9(a) presents both waveforms of PCC voltages for the system with MVQR compensation turned on and off. Fig. 9(b) and (c) shows the waveforms and the four components of reference i_{Lf}^{*} generated by the outer voltage loops. Finally, Fig. 9(d) shows harmonic spectrum of grid current (i_{gd}), load current (i_L) and converter current (i_c). Implementing the proposed scheme would reduce the component i_{90} of Fig. 9(c) to nearly zero and keep components

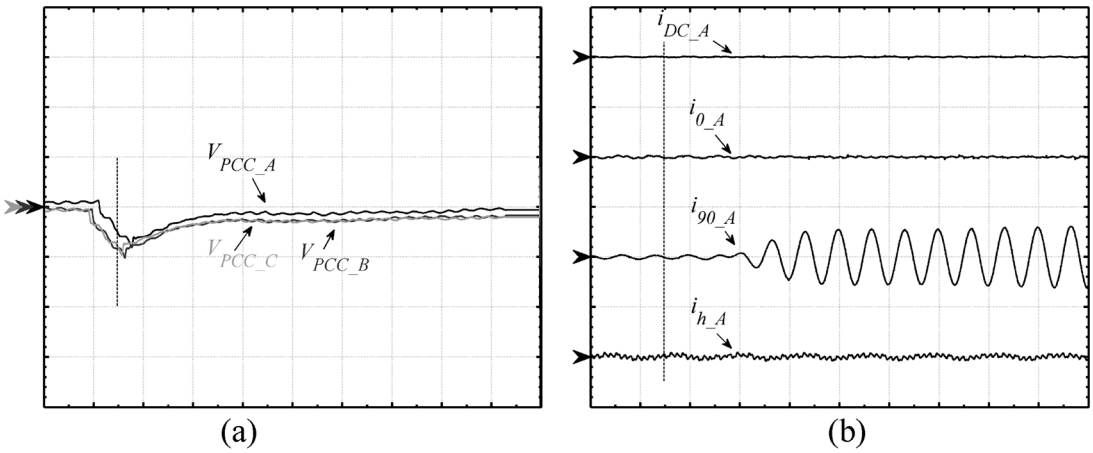

Fig. 10. Experimental results for load step in phase A. (a) rms voltages at v_{PCC} (ac coupling, 10 V/div, 25 ms/div). (b) Grid, load, and converter currents (40 A/div, 25 ms/div).

i_{DC}, i_0 and i_h unchanged. This will minimize the fundamental component of i_C in Fig. 9(b), and result in an amplitude reduction of i_{gd} and compensated voltage of Fig. 9(a) but keeping their compensated harmonic content. The effect of this will be to reduce the current circulation in the system during adequate voltage periods.

Table 4 shows the measured values with the existing MVRQ compensation turned off and on. One can observe from these results that proposed MVRQ compensation scheme compensates a distorted i_L by generating a compensation current i_c, resulting in a regulated PCC voltage with reduced distortion.

Fig. 10 presents experimental results for a linear load step (S_{lin1} = on, S_{lin2} = off, and S_{nlin} = off). First the system operates at steady state until instant t_1 when S_{lin2} is turned on. Fig. 10(a) shows that PCC rms voltage dropped to 210 V after the load step but the control action was fast enough to restore nominal value after approximately 100 ms. Fig. 10(b) shows that quadrature component of reference current i_{90} has its value modified by the transient, while the other references were kept unchanged. The implementation of the proposed scheme would result in a slow reduction of i_{90} amplitude, resulting in a slow reduction of V_{PCC}, but guarantying V_{PCC} amplitudes do not drop below $V_{rms\ \min}$.

5. Conclusion

A light control structure was added to a developed MVQR control structure, wisely adjusting PCC voltage setpoint to reduce unnecessary reactive power circulation supplied to the system. By using only available control signals, the control structure provided a reduction of processed reactive power towards to zero, of a three-phase converter, which can mitigate harmonics and adjust voltage levels in the PCC just after simply plugging into the power grid. A method was presented to analyze the impact of the proposed scheme for reduction of reactive energy injection which gives insights for it's design.

The results have shown a successful reduction of unnecessary reactive power circulation between the MVQR and the power distribution system under balanced and unbalanced system conditions, bringing the sum of the three phases' reactive power towards to zero and reducing the total reactive power processed by the MVQR while keeping output voltages balanced and within standards' limits. At the same time, MVQR capabilities like quick regulation PCC voltage magnitude, significant reduction of voltage harmonics and dc link voltage regulation remained unchanged.

Experimental results of the existing MVQR control scheme were presented and used to detail the effects of the proposed control scheme. Pointing out the MVQR internal signals changes with an implementation of the proposed control scheme, covering static and dynamic results. Thus, providing a wider view of the proposed solution.

Proposed scheme demonstrated itself as very effective in reducing MVRQ processed power while still complying with voltage regulation standards. The processed reactive power was approximately the minimal required to maintain all PCC voltages balanced within the acceptable voltage range. A simple method for reduction of processed reactive power was demonstrated, without the need of additional sensing of grid or load currents as well as not requiring grid parameters to determine the suitable PCC voltage magnitude.

The novel control scheme gives good results, presenting itself as a worthy implementation in similar systems as it uses very little resources and provides great benefits, especially in similar MVQT structures where signals proportional to output reactive power are decoupled.

References

[1] IEEE recommended practice and requirements for harmonic control in electric power systems, IEEE Std 519–2014 (Revision of IEEE Std 519–1992), pp. 1–29, June 2014.
[2] J. Rocabert, A. Luna, F. Blaabjerg, P. Rodríguez, Control of power converters in ac microgrids, IEEE Trans. Power Electron. 27 (November (11)) (2012) 4734–4749.
[3] A. Chandra, B. Singh, B. Singh, K. Al-Haddad, An improved control algorithm of shunt active filter for voltage regulation, harmonic elimination, power-factor correction, and balancing of nonlinear loads, IEEE Trans. Power Electron. 15 (May (3)) (2000) 495–507.
[4] Y.A.R.I. Mohamed, E. El-Saadany, A control scheme for pwm voltage-source distributed-generation inverters for fast load-voltage regulation and effective mitigation of unbalanced voltage disturbances, IEEE Trans. Ind. Electron. 55 (May (5)) (2008) 2072–2084.
[5] H. Akagi, New trends in active filters for improving power quality, Proceedings of the 1996 International Conference on Power Electronics, Drives and Energy Systems for Industrial Growth, January, 1996, vol. 1, 1996, pp. 417–425.
[6] P.-C. Tan, R. Morrison, D. Holmes, Voltage form factor control and reactive power compensation in a 25-kv electrified railway system using a shunt active filter based on voltage detection, IEEE Trans. Ind. Appl. 39 (March (2)) (2003) 575–581.
[7] J. Miret, M. Castilla, J. Matas, J. Guerrero, J. Vasquez, Selective harmonic-compensation control for single-phase active power filter with high harmonic rejection, IEEE Trans. Ind. Electron. 56 (August (8)) (2009) 3117–3127.
[8] P. Mattavelli, F. Marafao, Repetitive-based control for selective harmonic compensation in active power filters, IEEE Trans. Ind. Electron. 51 (October (5)) (2004) 1018–1024.
[9] R. Costa-Castello, R. Grino, E. Fossas, Odd-harmonic digital repetitive control of a single-phase current active filter, IEEE Trans. Power Electron. 19 (July (4)) (2004) 1060–1068.
[10] G. Weiss, Q.-C. Zhong, T. Green, J. Liang, H^{∞} repetitive control of dc-ac converters in microgrids, IEEE Trans. Power Electron. 19 (January (1)) (2004) 219–230.
[11] H. Akagi, Control strategy and site selection of a shunt active filter for damping of harmonic propagation in power distribution systems, IEEE Trans. Power Deliv. 12 (January (1)) (1997) 354–363.
[12] F. Freijedo, J. Doval-Gandoy, O. Lopez, P. Fernandez-Comesana, C. Martinez-Penalver, A signal-processing adaptive algorithm for selective current harmonic cancellation in active power filters, IEEE Trans. Ind. Electron. 56 (August (8)) (2009) 2829–2840.
[13] H. Akagi, H. Fujita, K. Wada, A shunt active filter based on voltage detection for harmonic termination of a radial power distribution line, Industry Applications

Conference, 1998. Thirty-Third IAS Annual Meeting. The 1998 IEEE, October, vol. 2, 1998, pp. 1393–1399.
[14] M. Salo, H. Tuusa, A novel open-loop control method for a current source active power filter, IEEE Trans. Ind. Electron. 50 (April (2)) (2003) 313–321.
[15] Y. Sato, H. Chigira, T. Kataoka, A new control method for active power filters with voltage detection, Proceedings of the Power Conversion Conference, Nagaoka, August, 1997, vol. 1, 1997, pp. 169–174.
[16] H. Akagi, Active harmonic filters, Proc. IEEE 93 (December (12)) (2005) 2128–2141.
[17] M. Aredes, L.F.C. Monteiro, A control strategy for shunt active filter, 10th International Conference on Harmonics and Quality of Power, October, 2002, vol. 2, 2002, pp. 472–477.
[18] Y. Sato, T. Kawase, M. Akiyama, T. Kataoka, A control strategy for general-purpose active filters based on voltage detection, IEEE Trans. Ind. Appl. 36 (September (5)) (2000) 1405–1412.
[19] H. Fujita, H. Akagi, Voltage-regulation performance of a shunt active filter intended for installation on a power distribution system, IEEE Trans. Power Electron. 22 (May (3)) (2007) 1046–1053.
[20] T. Geury, S. Pinto, J. Gyselinck, Current source inverter-based photovoltaic system with enhanced active filtering functionalities, IET Power Electron. 8 (December (12)) (2015) 2483–2491.
[21] F.H.M. Rafi, M.J. Hossain, J. Lu, Improved neutral current compensation with a four-leg PV smart VSI in a LV residential network, IEEE Trans. Power Deliv. 32 (October (5)) (2017) 2291–2302.
[22] R.K. Agarwal, I. Hussain, B. Singh, Implementation of LLMF control algorithm for three-phase grid-tied SPV-DSTATCOM system, IEEE Trans. Ind. Electron. 64 (September (9)) (2017) 7414–7424.
[23] M. Aggarwal, S.K. Gupta, M. Madhusudan, G. Kasal, D-statcom control in low voltage distribution system with distributed generation, 2010 3rd International Conference on Emerging Trends in Engineering and Technology (ICETET), November, 2010, pp. 426–429.
[24] B. Singh, A. Adya, A. Mittal, J.R.P. Gupta, Analysis, simulation and control of dstatcom in three-phase, four-wire isolated distribution systems, Power India Conference, 2006 IEEE (2006) p. 6.
[25] A. Etemadi, R. Iravani, Overcurrent and overload protection of directly voltage-controlled distributed resources in a microgrid, IEEE Trans. Ind. Electron. 60 (December (12)) (2013) 5629–5638.
[26] C. Gehrke, A. Lima, A. Oliveira, Controlling harmonics in electrical power systems for satisfying total and individual harmonic distortion constraints, Applied Power Electronics Conference and Exposition (APEC), 2014 Twenty-Ninth Annual IEEE, March, 2014, pp. 3342–3348.
[27] J. He, Y.W. Li, F. Blaabjerg, X. Wang, Active harmonic filtering using current-controlled, grid-connected dg units with closed-loop power control, IEEE Trans. Power Electron. 29 (February (2)) (2014) 642–653.
[28] C. Kumar, M. Mishra, A multifunctional dstatcom operating under stiff source, IEEE Trans. Ind. Electron. 61 (July (7)) (2014) 3131–3136.
[29] R. Mastromauro, M. Liserre, A. Dell'Aquila, Control issues in single-stage photovoltaic systems: MPPT, current and voltage control, IEEE Trans. Ind. Inform. 8 (May (2)) (2012) 241–254.
[30] Y.A.R.I. Mohamed, E. El-Saadany, Hybrid variable-structure control with evolutionary optimum-tuning algorithm for fast grid-voltage regulation using inverter-based distributed generation, IEEE Trans. Power Electron. 23 (May (3)) (2008) 1334–1341.
[31] Y.-R. Mohamed, Mitigation of dynamic, unbalanced, and harmonic voltage disturbances using grid-connected inverters with lcl filter, IEEE Trans. Ind. Electron. 58 (September (9)) (2011) 3914–3924.
[32] B. Singh, S.R. Arya, A. Chandra, K. Al-Haddad, Implementation of adaptive filter in distribution static compensator, IEEE Trans. Ind. Appl. vol. 50, (September–October (5)) (2014) 3026–3036.
[33] C. Kumar, M. Mishra, An improved hybrid dstatcom topology to compensate reactive and nonlinear loads, IEEE Trans. Ind. Electron. 61 (December (12)) (2014) 6517–6527.
[34] R.T. Hock, Y.R. De Novaes, A.L. Batschauer, A voltage regulator based in a voltage-controlled dstatcom with minimum power point tracker, Energy Conversion Congress and Exposition (ECCE), 2014 IEEE, September, 2014, pp. 3694–3701.
[35] C. Kumar, M. Mishra, A voltage-controlled dstatcom for power quality improvement, IEEE Trans. Power Deliv. 29 (June (3)) (2014) 1499–1507.
[36] T.-L. Lee, S.-H. Hu, Discrete frequency-tuning active filter to suppress harmonic resonances of closed-loop distribution power systems, IEEE Trans. Power Electron. 26 (January (1)) (2011) 137–148.
[37] C. Kumar, M. Mishra, Operation and control of an improved performance interactive dstatcom, IEEE Trans. Ind. Electron. 62 (October (10)) (2015) 6024–6034.
[38] S.-L. Jung, H.-S. Huang, M.-Y. Chang, Y.-Y. Tzou, Dsp-based multiple-loop control strategy for single-phase inverters used in ac power sources, Power Electronics Specialists Conference, 1997. PESC '97 Record., 28th Annual IEEE, June, vol. 1, 1997, pp. 706–712.
[39] A. Yepes, F. Freijedo, J. Doval-Gandoy, O. Lopez, J. Malvar, P. Fernandez-Comesana, On the discrete-time implementation of resonant controllers for active power filters, Industrial Electronics, 2009. IECON '09. 35th Annual Conference of IEEE, November, 2009, pp. 3686–3691.
[40] ANSI C84. 1-2011, Electric Power Systems and Equipment — Voltage Ratings (60 Hertz), NEMA, United States of America, 2011.
[41] EN 50160, Voltage Characteristics of Electricity Supplied by Public Distribution Systems, CENELEC, Brussels, Belgium, 2005.
[42] M. Mishra, A. Ghosh, A. Joshi, Operation of a DSTATCOM in voltage control mode, IEEE Trans. Power Deliv. 18 (January (1)) (2003) 258–264.
[43] C. Kumar, M. Mishra, Energy conservation and power quality improvement with voltage controlled DSTATCOM, Proceedings of the 2013 Annual IEEE India Conference (INDICON), December, 2013, pp. 1–6.
[44] R.T. Hock, Y.R. de Novaes, A.L. Batschauer, A voltage regulator for power quality improvement in low-voltage distribution grids, IEEE Trans. Power Electron. 33 (March (3)) (2018) 2050–2060.
[45] C. Kumar, M.K. Mishra, M. Liserre, Design of external inductor for improving performance of voltage-controlled DSTATCOM, IEEE Trans. Ind. Electron. 63 (August (8)) (2016) 4674–4682.
[46] R. Abbassi, S. Marrouchi, M.B. Hessine, H. Jouini, S. Chebbi, Voltage control strategy of an electrical network by the integration of the UPFC compensator, Int. Rev. Model. Simul. 5 (1) (2016) 380–384.
[47] P. Chittora, A. Singh, M. Singh, Simple and efficient control of DSTATCOM in three-phase four-wire polluted grid system using MCCF-SOGI based controller, IET Gener. Transm. Distrib. 12 (March (5)) (2018) 1213–1222.
[48] S. Saidi, R. Abbassi, S. Chebbi, Fuzzy logic controller for three-level shunt active filter compensating harmonics and reactive power, Int. J. Adapt. Control Signal Process. 30 (6) (2016) 809–823.
[49] M. Mangaraj, A.K. Panda, Performance analysis of DSTATCOM employing various control algorithms, IET Gener. Transm. Distrib. 11 (10) (2017) 2643–2653.
[50] H. Myneni, G. Siva Kumar, D. Sreenivasarao, Dynamic dc voltage regulation of split-capacitor DSTATCOM for power quality improvement, IET Gener. Transm. Distrib. 11 (November (17)) (2017) 4373–4383.
[51] J.C. da Cunha, S.V.G. Oliveira, L. Michels, M. Mezaroba, Multifunctional current-controlled DSTATCOM with harmonic mitigation through voltage detection, 2015 IEEE International Conference on Industrial Technology (ICIT), Seville, 2015, pp. 1348–1354.